

## Polymer Brushes with Liquid Crystalline Side Chains

Bin Peng, Diethelm Johannsmann, and Jürgen Rühle\*

Max-Planck-Institute for Polymer Research, Ackermannweg 10, D-55128 Mainz, Germany

Received September 16, 1998; Revised Manuscript Received June 15, 1999

**ABSTRACT:** We report on the synthesis and the properties of side-chain liquid-crystal polymer (LCP) brushes attached to silicon oxide surfaces. The polymer monolayers have been generated at the surface of the substrate in situ following a “grafting-from” procedure. The mesogenic group of the LC brushes consists of a phenylbenzoate moiety linked to the methacrylate main chain via a flexible spacer. The thickness of the brush and the grafting density of the surface-attached polymer molecules can be controlled by adjusting the monomer concentration during brush growth and the reaction time of the polymerization, respectively. LC brushes with a thickness of up to 200 nm in the dry, solvent-free state have been obtained. The transition temperatures between the nematic and the isotropic state have been studied and compared to those of spin-cast films of the same polymer. The optical textures are investigated as a function of layer thickness, temperature, and sample history. The textures exhibit a strong memory effect in the sense that the exact same texture reappears after isotropization by heating or solvent exposure and returning to the nematic state.

### Introduction

Alignment layers are key components for the production of liquid-crystal (LC) displays.<sup>1–4</sup> Most frequently, rubbed polymer films, in particular polyimides, are used to orient low molecular weight liquid crystals in such a display into macroscopic domains. For this purpose, thin films of the polymers are coated onto the surfaces of the LC cells. After mechanical treatment, the polymer-coated surfaces are brought into contact with the LC material. They orient the (low molecular weight) liquid crystalline molecules along the rubbing direction. For optimum operation of the display, a tilt of the LC director with respect to the aligning surface is needed.<sup>5</sup> This is particularly important for supertwisted nematic (STN) displays where pretilt angles of more than 10° are required. The introduction and the control of high pretilt angles remains a problem also for the introduction of various new display schemes.

D. R. Williams and A. Halperin have suggested the use of LCP brushes as high-tilt alignment layers.<sup>6,7</sup> In such systems, the chains of the LC polymer are covalently attached to the substrate at one end. If the grafting density of the surface-attached chains is high enough, the overlap between neighboring chains results in chain stretching away from the surface to a brushlike conformation.<sup>8–10</sup> The purpose of the brush is to induce a certain orientation of the nematic director in the adjacent bulk liquid-crystal (LC) phase. Interestingly, this orientation could be tilted because there may be a competition between the orienting action of the stretched polymer chains and the uncovered fraction of the substrate. Williams and Halperin considered main-chain LCP brushes on a polar substrate. In this case, the bare substrate induces an LC alignment parallel to the surface, while the chains stretched away from the surface favor perpendicular (homeotropic) orientation. The competition between these two effects can be tuned via the surface coverage of the brush component. A second-order tilting transition as a function of grafting density is predicted, which leads to tilted orientations close the critical point. In principle, alignment due to the brush-type conformation should be also present in

side-chain LCPs, although the effect may be weaker, depending on the degree of coupling between the main-chain and side-chain orientation (Figure 1).

With side-chain LCP brushes it is expected that there is a competition between chain stretching and the aligning action of the uncovered surface if the latter is modified such that it induces perpendicular (homeotropic) orientation. This can be achieved by coating it with substances containing flexible alkyl chains. Since it is well-known that the nematic director in side-chain LC polymers is coupled to the orientation of the polymer backbone,<sup>11,12</sup> we expect to find an influence of main-chain stretching induced by the brush topology. In our case, we expect the backbones to be preferentially aligned perpendicular to the substrate surface. As a consequence, the interaction with the surface should differ between brushes and spin-cast films.

In this paper we report on the preparation of side-chain LCP brushes. Side-chain LCPs were chosen because it is less difficult in such systems to find low molecular weight nematic LCs miscible with the polymer. Swelling of the brush in the bulk nematic medium, however, is according to the mechanism described above a prerequisite for the functioning of an LC brush as an alignment layer. The polymer monolayers described here were prepared by the “grafting-from” technique.<sup>13,14</sup> The polymer chains are grown in situ by free chain radical polymerization from an initiator which is covalently attached to the surface of a substrate. The polymer monolayers obtained in this way are much thicker than the layers obtained by immobilizing preformed functionalized polymers because no diffusion of entire chains toward the substrate is required as in case of “grafting-to” procedures. The optical textures and the transition temperatures found for the brushes are compared to the ones found for spin-cast films from the same polymer.

### Experimental Section

**Synthesis of the Monolayers.** Synthesis of the monomer (“M6” for short) was carried out in a manner similar to that described in ref 15. It is obtained through a base-catalyzed etherification of *p*-hydroxybenzoic acid with  $\omega$ -chlorohexanol

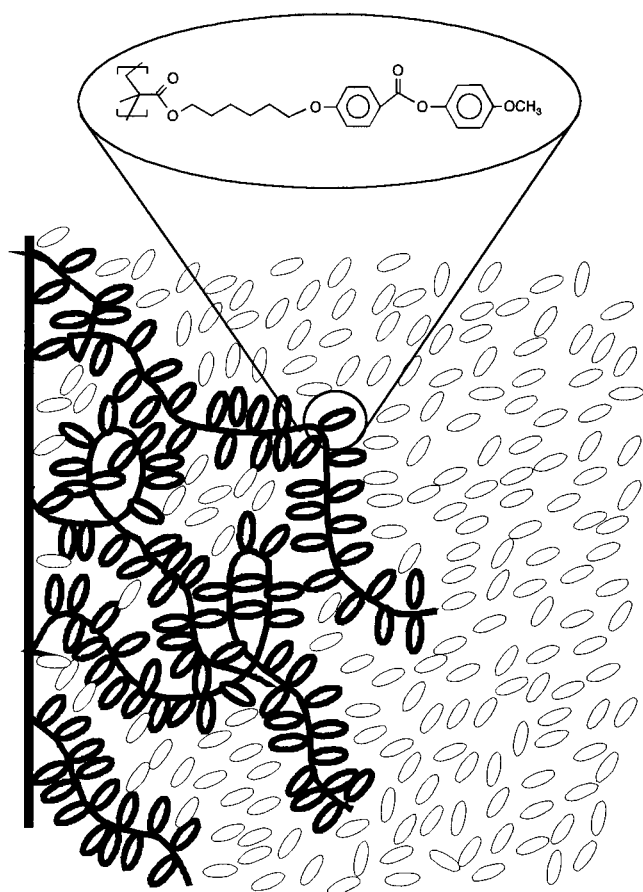


**Figure 1.** Schematic depiction of an LC brush swollen in a low molecular weight nematic. Competing orienting actions from the brush and the bare surface may result in a tilted alignment. The chemical structure of the mesogen used in this study is indicated in the inset.

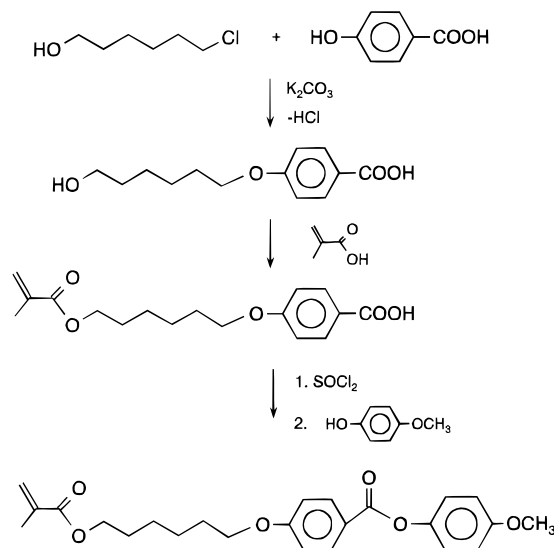


**Figure 2.** Outline of the monomer synthesis.

and subsequent esterification of the product with methacrylic acid, transformation into the acid chloride, and reaction with *p*-hydroxyanisole. A schematic outline of the synthetic procedures is shown in Figure 2. Compared to ref 15, the purification of the final product was somewhat modified. Impurities in the methacrylate monomer were removed by column chromatography (silica gel, 1:80 (by weight); eluent *n*-hexane:ethyl acetate = 5:2) and subsequent recrystallization from 2-propanol.

**Table 1.** Properties of Bulk LC Polymer Materials

sample code	initiator concn (mol %)	polym time (h)	$M_n^a$	$M_w^a$	$M_w/M_n$	$T_{NI}^b$ (°C)
PM6-3	0.68	8.5	156 000	600 000	3.85	111.1
PM6-2	1.0	10.5	79 000	249 000	3.15	110.8
PM6-4	2.0	7.2	56 400	128 000	2.27	110.9

<sup>a</sup> Molecular weights measured by GPC; eluent THF; calibration with PMMA standards. <sup>b</sup>  $T_{NI}$  was measured with a polarizing microscope.

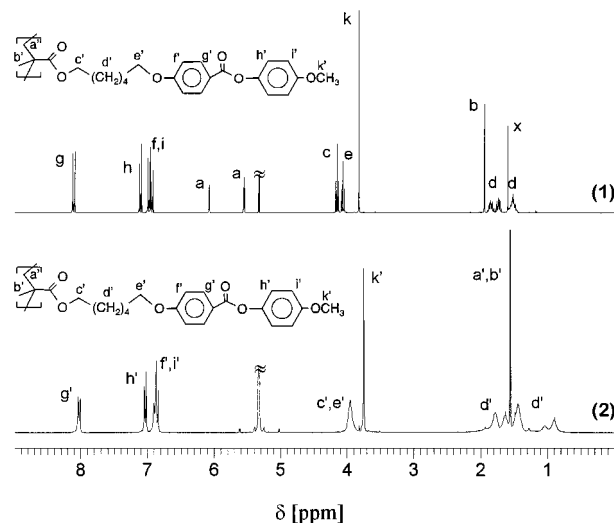


**Figure 3.**  $^1\text{H}$  NMR spectra (300 MHz,  $\text{CD}_2\text{Cl}_2$ ) of the monomer (spectrum 1) and LC polymer (spectrum 2).

$^1\text{H}$  NMR ( $\text{CD}_2\text{Cl}_2$ ,  $\delta$  in ppm):<sup>28</sup> 1.53 (q, 4H); 1.72 (q, 2H); 1.85 (q, 2H); 1.93 (s, 3H); 3.82 (s, 3H); 4.06 (t, 2H); 4.14 (t, 2H); 5.55 (s, 1H); 6.08 (s, 1H); 6.96 (dd, 4H); 7.10 (d, 2H); 8.11 (d, 2H).

$^{13}\text{C}$  NMR ( $\text{CD}_2\text{Cl}_2$ ,  $\delta$  in ppm): 18.39; 26.01; 26.12; 28.91; 29.35; 55.91; 64.88; 68.59; 114.63; 114.72; 122.13; 122.90; 125.01; 132.39; 137.13; 145.01; 157.68; 163.86; 165.49; 167.61.

To compare the properties of the LCP brushes with the properties of spin-cast films, we also produced bulk LCP material from the same monomer under similar polymerization conditions. However, a conventional (i.e., not surface-attached) initiator, namely azobis(isobutyronitrile) (AIBN), was used. The polymerizations were carried out at 60 °C under inert atmosphere in toluene. The initiator concentration was chosen between 0.5 and 2 mol %. Polymerization times were 7–11 h (Table 1).

$^1\text{H}$  NMR ( $\text{CD}_2\text{Cl}_2$ ,  $\delta$  in ppm): 1.45–1.90 (m, 8H); 1.62 (s, 3H); 3.75 (s, 3H); 3.82–4.04 (b, 4H); 6.84–7.09 (m, 6H); 8.10 (d, 2H).

$^{13}\text{C}$  NMR ( $\text{CD}_2\text{Cl}_2$ ,  $\delta$  in ppm): 17 (b); 19 (b); 26.13; 26.36; 28.53; 29.46; 45.3 (b); 55.93; 65.30; 68.61; 114.66; 114.75; 122.22; 122.93; 132.45; 145.01; 157.70; 163.82; 165.42; 178 (b).

Figure 3 shows the  $^1\text{H}$  NMR spectra of the monomer and the bulk polymer, which demonstrate that both compounds could be obtained in a pure form.<sup>29</sup> The properties of the different bulk LCP materials are given in Table 1. Spin-coated films were prepared with polymer PM6-4 dissolved in dichloromethane (8.4 mg/mL). The speed of rotation was between 600 and 2000 rpm. The thickness of the layers was between 56 and 104 nm.

The formation of the polymer brushes is achieved by growing the polymer chains directly at the surface of the substrate using a surface-attached initiator<sup>16,17</sup> as depicted in Figure 4. Briefly, the first step is the immobilization of the initiator for the free radical polymerization onto the substrate. The initiator is a derivative of AIBN containing two monochlorosilyl moieties. One of them is attached to the substrate via a base catalyzed condensation reaction with the surface hydroxyl groups of the silicon oxide substrate. We have shown that the

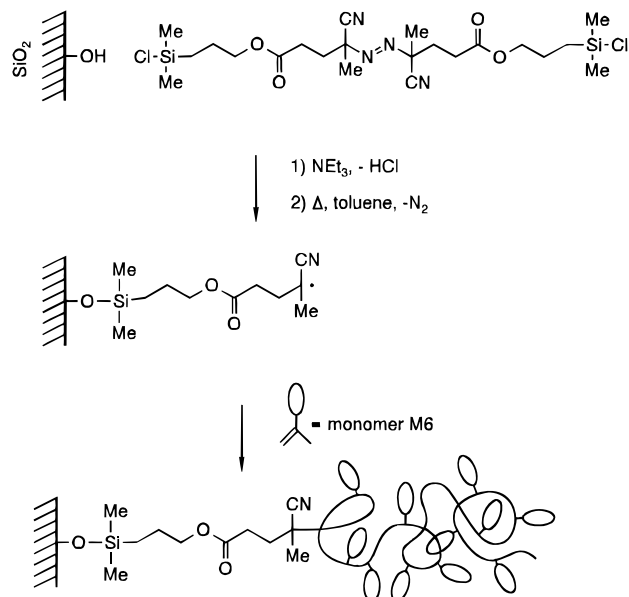


**Figure 4.** Schematic description of the growth of LC polymers at the surface of a substrate.

bidentate initiator used here can be attached to the surface either just on one side or on both ends, depending on the reaction conditions. However, apart from slight changes of the molecular weight of the surface-attached polymers this does not influence the formation of the brush strongly. In a second step the polymerization of the LC monomer is carried out at 60 °C. Toluene is used as a solvent in all cases. All solutions were carefully degassed before polymerization during at least three freeze–thaw cycles. As substrates we used BK7 glass slides (Schott) either directly as obtained or coated with a 30 nm thick layer of evaporated  $\text{SiO}_x$  on top of a thin (50 nm) silver film. The latter substrates are needed for the determination of monolayer thickness with surface plasmon spectroscopy (SPS). We usually prepared two samples with a bare glass substrate and an  $\text{SiO}_x$  surface in the same reaction vessel. We assume that the polymer film thickness on the  $\text{SiO}_x$  sample is similar to the thickness of the brush on the glass surface, which is difficult to determine directly. After polymerization, the samples are rinsed with solvents and undergo Soxhlet extraction with toluene for 15 h to remove physisorbed polymer.

The molecular weight of the LC brushes is a priori unknown. However, we have shown that the molecular weight and molecular weight distribution of the surface-attached chains and that of the “free” polymer formed during brush growth are under many experimental conditions identical.<sup>17</sup> GPC-analysis of the “free” polymer formed during the surface polymerization reactions showed that, depending on reaction conditions and monomer concentration, chains with a molecular weight of 200 000 to 1 000 000 had been formed. The polydispersity  $M_w/M_n$  of all samples ranged between 1.5 and 2.

**Instrumental.** The liquid-crystal textures were studied with a Zeiss-Axiophot polarization microscope equipped with a Linkam TH600 hot stage. The integrated transmitted intensity through samples on glass slides was measured as a function of temperature with a photometer integrated into the camera. The transition temperatures were derived from both visual inspection of the texture and the integrated transmission. The two procedures yielded identical results. The heating rate typically was about 0.2 °C/min near the transition. All measurements of the transition temperatures were repeated at least three times and were reproducible within 0.1 °C.

Surface plasmon and optical waveguide spectroscopy measurements were carried out in the conventional ATR configuration (Figure 7a) at a wavelength of 633 nm.<sup>18</sup> The laser light was coupled through a prism into the sample consisting of a glass substrate, onto which 50 nm of silver and 30 nm of

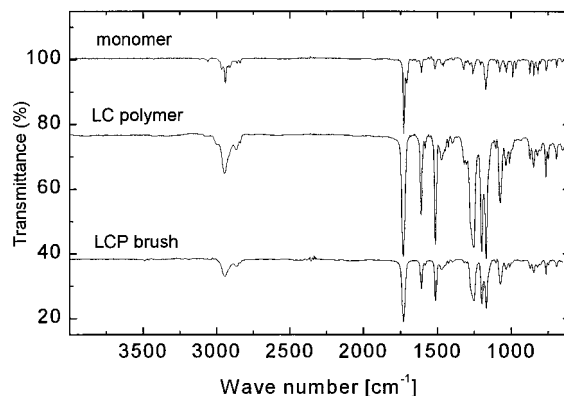


**Figure 5.** Transmission IR spectra of monomer, bulk polymer, and a polymer brush attached to both faces of a silicon wafer.

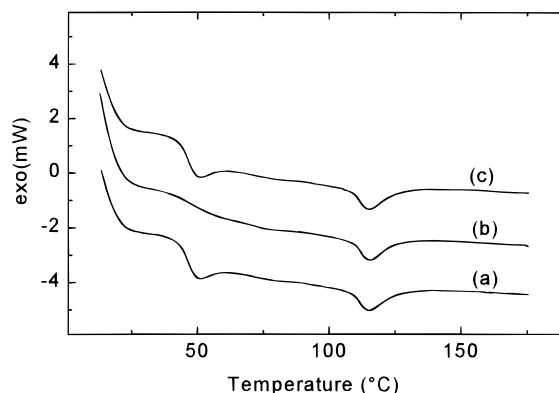


**Figure 6.** DSC data obtained on the free polymer: (a) first heating cycle; (b) same sample as part a measured directly after cooling back to room temperature; (c) same sample as part b after 1 day storage at room temperature. Curves b and c have been displaced for clarity.

$\text{SiO}_x$  had been evaporated. The sample cell was mounted on a  $\theta/2\theta$  goniometer having an angular accuracy of 0.01°. The intensity of the reflected light was measured as a function of the incident angle. All measurements were repeated at least three times on different locations of the sample.

IR spectra were recorded using a nitrogen purged Nicolet Omnic 850 spectrometer. Transmission spectra of the LC brushes were measured using 1 mm thick silicon wafers polished on both faces (Aurel) as substrates. Typically 1000 scans were accumulated with a resolution of 4  $\text{cm}^{-1}$ . DSC measurements were carried out using a DSC7 system from Mettler. The heating and cooling rates were 10 K/min.

## Results and Discussions

LC polymer monolayers were obtained by thermally initiated polymerization reactions using the immobilized azoinitiator. It should be noted that all monolayers discussed in the following have been extracted for at least 15 h in a Soxhlet extractor with toluene, which is a good solvent for the polymer. Reference experiments with spin-cast films, where the polymer is only physically adsorbed to the surface, showed that such an extraction procedure removes all physisorbed polymer.

Figure 5 shows transmission FTIR spectra of the monomer, the bulk polymer and a polymer monolayer attached to a silicon substrate. The good agreement of the spectra of the brush-coated substrate and the free polymer, concerning both characteristic absorption bands (C–H and carbonyl vibrations at 1730 and 2944  $\text{cm}^{-1}$  respectively) and absorption bands in the fingerprint region of the spectrum, proves that indeed the desired

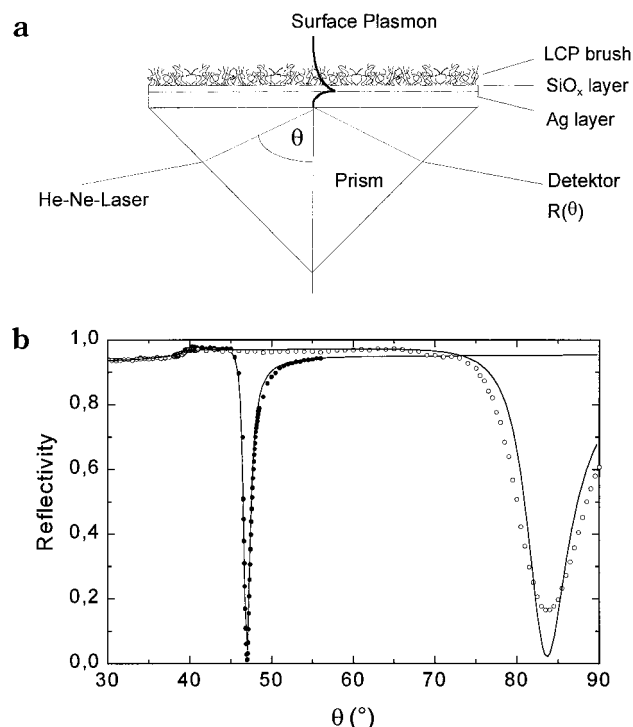


**Figure 7.** (a) Schematic depiction of the surface plasmon spectroscopy (SPS) experiment. (b) Reflectivity of a surface plasmon substrate before surface modification (●) and after growth of the brush and Soxhlet extraction (○). The straight lines are calculated reflectivities using the Fresnel theory.

LC brush has been formed during the surface polymerization reaction.

To understand the thermal behavior of the polymer differential scanning calorimetry (DSC) experiments on the bulk LC polymer were carried out (Figure 6). The step at about 50 °C is assigned to the glass transition of the bulk polymer. This interpretation is corroborated by observations on the dynamics of domain formation under the polarization microscope in spin-cast films and brushes (see below). Directly after preparation, spin-cast films and LCP brushes are found to be isotropic. The nematic textures gradually appear when annealing the sample at 50 °C or above. In the first heating cycle (Figure 6, trace a) there is a pronounced endothermic signal around 50 °C which can be attributed to the melting of crystalline domains in the films. If the sample is cooled rapidly, the signal is not present in the subsequent heating cycle (trace b). However, it reappears when the sample is kept at room temperature for 1 day (trace c). Thermal gravimetric measurements (TGA) (not shown) indicate that the polymer is thermally stable up to 280 °C, and no degradation occurs under the conditions used here ( $T < 160$  °C).

**Brush Thickness.** We determined the thickness of the brushes in the dry, collapsed state with surface plasmon spectroscopy.<sup>18</sup> Figure 7a shows the principle of the measurement. The brush thickness is inferred from the position of the sharp dip (surface plasmon) in the reflectivity at the resonance angle (Figure 7b). A dielectric layer on the metal surface shifts the surface plasmon resonance signal toward higher angles of incidence compared to that of the unmodified substrate. The full dots show the reflectivity curve of the bare substrate prior to the experiment. Open dots correspond to the plasmon after polymerization and Soxhlet extraction. Modeling the data with the Fresnel equations

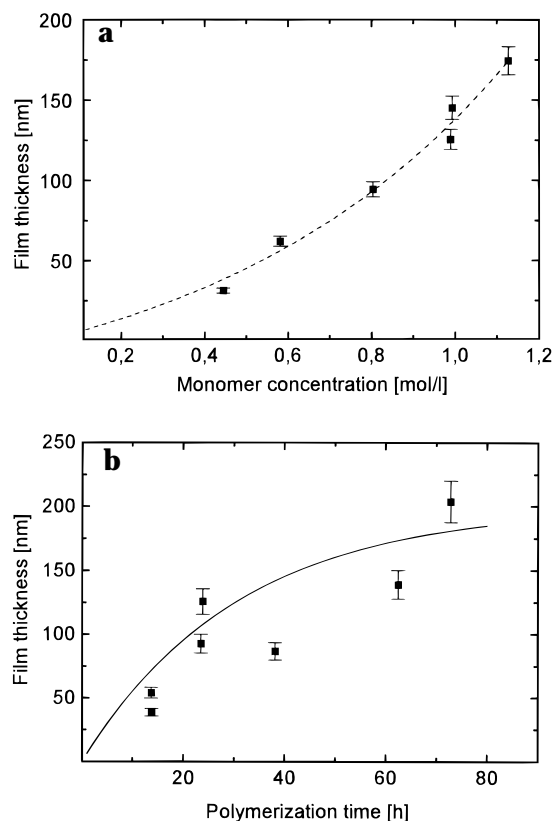


**Figure 8.** (a) Thickness of the LC monolayers as a function of monomer concentration during polymerization:  $T = 60$  °C;  $t = 24$  h. (b) Dependence of brush thickness on polymerization time:  $T = 60$  °C;  $[M] = 0.8$  mol/L.

using a simple box model yields a brush thickness of 61.6 nm. For thin films the analysis requires an assumption on the refractive index of the surface-attached polymer, which was obtained from waveguide spectra of thicker films as  $n = 1.587$ . Washing and extraction of spin-cast films in the same way results in complete removal of the LCP.

Figure 8a displays the brush thicknesses after extraction as a function of monomer concentration during brush growth. The polymerization time was 24 h in all cases. The data points are averages from at least three different spots on the samples. The error bars indicate the variation of thickness across the sample surface. Figure 8b shows the dependence of the brush thickness on the polymerization time. The monomer concentration was kept fixed at 0.80 M for this data set.

The increase of brush thickness with monomer concentration (Figure 8a) is largely caused by an increase in molecular weight of the surface-attached polymer as the molecular weight of polymers during radical chain polymerization is proportional to the first power of the monomer concentration.<sup>19</sup> The deviation from a linear slope is due to transfer to solvent (toluene) as it has been shown for the formation of brushes of the unsubstituted PMMA.<sup>17</sup> The grafting density of the chains tethered to the surface, on the other hand, is mostly a function of polymerization time as long as other parameters (e.g., temperature and graft density of the initiator) are kept constant. With increasing reaction time, the number of decomposed initiator molecules and accordingly the number of formed polymer chains increases leading to a corresponding increase in film thickness (Figure 8b). By adjustment of the monomer concentration and polymerization time, monolayers of the LC polymers with



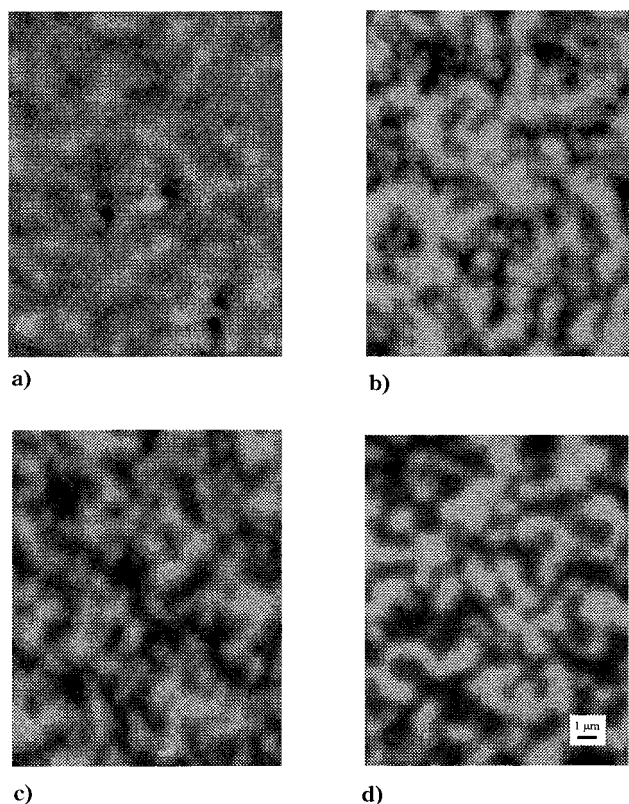


**Figure 9.** Liquid-crystal textures obtained for polymer brushes of varying thicknesses  $d$ : (a)  $d = 38$  nm; (b)  $d = 61$  nm; (c)  $d = 86$  nm; (d)  $d = 126$  nm.

thicknesses ranging from a few nanometers to more than 200 nm can be obtained.

**Textures.** Immediately after drying, the LCP brushes appear dark between crossed polarizers. Apparently, they have been quenched into an isotropic state. When heated to the glass transition temperature,  $T_g \sim 50$  °C (cf. Figure 6), a nematic texture slowly appears. Although the LC brushes are monolayers in the direct sense, i.e., one single layer of (polymer) molecules attached to the surface, the layers are thick enough to allow for the optical observation of textures.

Pictures of LC textures at different temperatures were taken after holding the sample at a constant temperature for at least 3 min. Figure 9 shows the textures of brushes with thicknesses of 38 (a), 61 (b), 81 (c), and 126 nm (d). Even for a brushes as thin as 38 nm one finds a liquid-crystal texture with a lateral length scale in the range of some micrometers (Figure 9a). Apparently, the film thickness is not the natural length scale of the lateral pattern of nematic orientation.

Figure 10 shows a sequence of textures obtained on the sample with a thickness of 126 nm at temperatures of 22 (a), 100 (b), 113 (c), and 113.7 °C (d). The N–I transition occurs at  $113.7 \pm 0.1$  °C. For temperatures below 112 °C (parts a and b of Figure 10) the texture is different from the well-known schlieren or thread textures usually observed for nematics. Different domains are frequently separated by dark lines. One observes neither a line ending anywhere nor a junction of an odd number of lines. This behavior is typical of topological defect lines.<sup>20</sup> Although we do not know the exact nature of the defects structures, we believe them to be related to disclination walls originating from conflicting boundary conditions at the top and the bottom interfaces. Presumably, the film–air interface

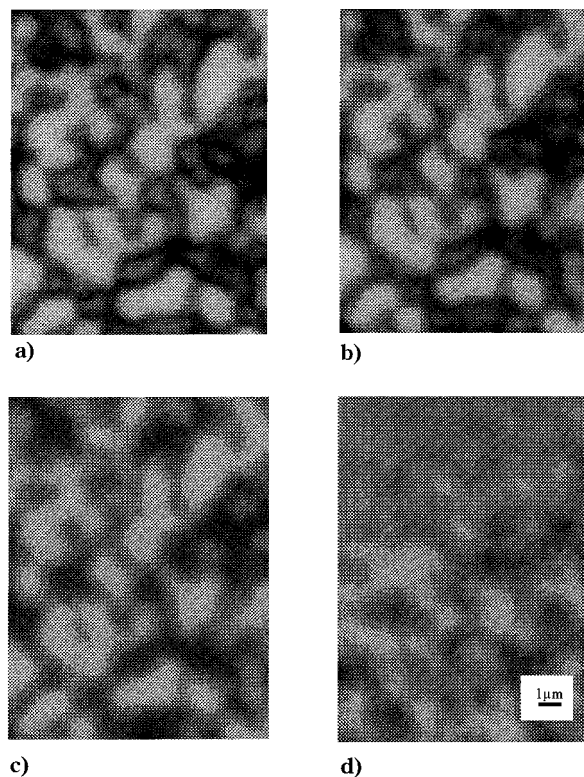


**Figure 10.** Liquid-crystal textures obtained for polymer brushes (thickness = 126 nm) at temperatures of 22 (a), 100 (b), 113 (c), and 113.7 °C (d).  $T_{NI} = 113.7 \pm 0.1$  °C. The dark lines (disclination walls) disappear immediately below  $T_{NI}$ .

imposes homeotropic alignment, while the substrate favors parallel alignment. The latter fact was proven by with LC cells, where the cell surfaces were covered with a surface-attached initiator, which was thermally decomposed in the absence of monomer. Since no monomer was present, no brush was formed, and the surface mimics the surface chemistry found between the anchor points of surface-attached chains. On these surfaces, a low molecular weight liquid crystal (1:2 mixture of *p*-pentylphenyl *p*-(hexyloxy)benzoate and *p*-pentylphenyl *p*-methoxybenzoate; ZLI 1052 Merck KGaA) revealed parallel orientational anchoring. This kind of conflicting anchoring is quite common for thin films and has been used to study the phase behavior of low molecular weight liquid crystals under strong orientational stress.<sup>21</sup> Under this assumption the nematic director in the brush undergoes a splay–bend distortion in order to accommodate both boundary conditions. The sense of rotation in this distortion may take two different signs. Domains with a different sense of rotation cannot be continuously connected to each other. The boundary is a topological defect. Close to these disclination walls the nematic order is reduced, which makes them appear as dark lines. In the future, we plan to further investigate this topic by coadsorbing alkyl chains with the initiator. Alkyl chains are known to induce homeotropic alignment. The varying boundary conditions should profoundly affect the director profile.

Interestingly, the lines disappear close to the N–I transition (Figure 10c). Possibly this is the consequence of an underlying homeotropic-to-homogeneous anchoring transition at the film–air interface. Such an anchoring transition driven by a change in order parameter has been observed before.<sup>22,23</sup> Figure 10d shows the coexistence between the LC and the isotropic phases at



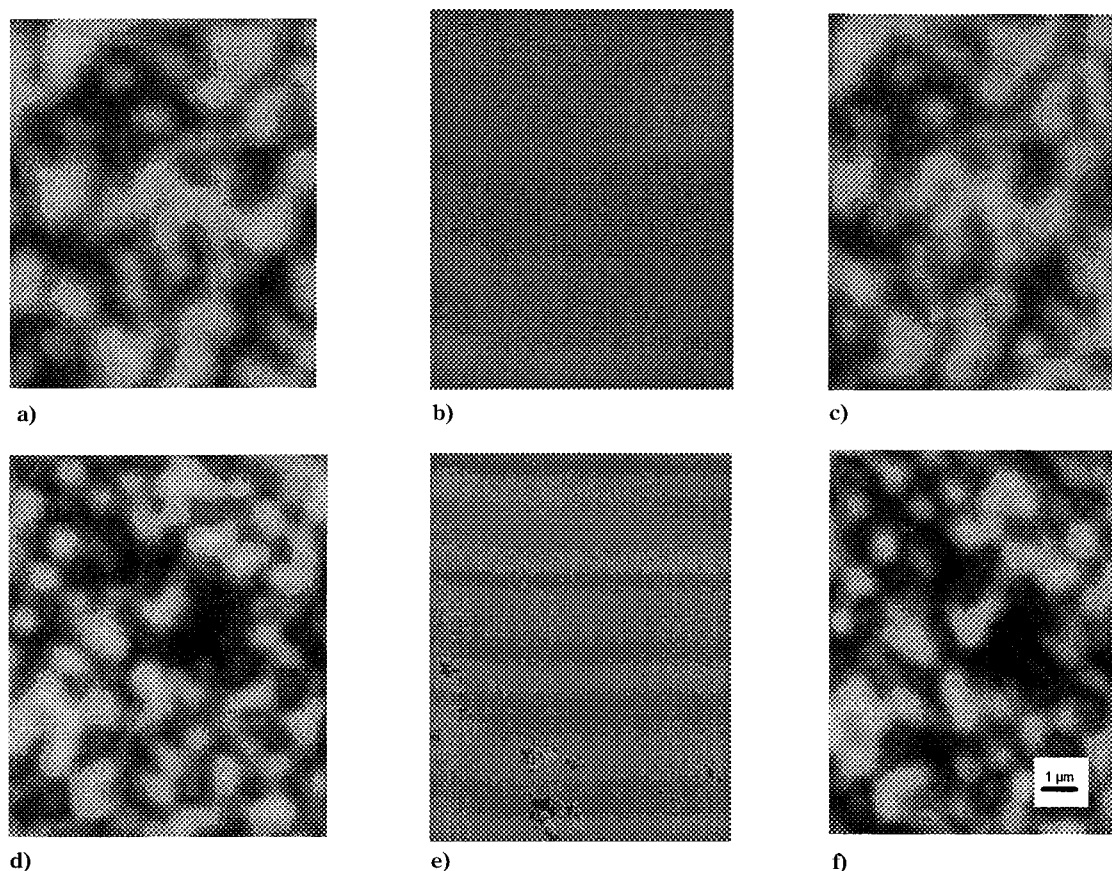


**Figure 11.** Surface memory effect of LCP brushes (sample B126). The sample shown in part a was heated to the isotropic phase (b) ( $T = 120\text{ }^{\circ}\text{C}$ ,  $t = 30\text{ min}$ ) and then returned back to the LC state by cooling (c). Pictures d and f were taken before and after the sample had been immersed into  $\text{CH}_2\text{Cl}_2$ , which is a good solvent for the brushes, for 2 h. During solvent exposure the LC structure was completely destroyed (e). After drying and annealing the sample showed the identical LC textures (f) as before solvent exposure (d).

$113.7\text{ }^{\circ}\text{C}$ , which proves that the N–I transition in the brush system is a first-order process and that the LC brush is obtained in a very pure form.

The observed textures do not vary with time even if the LCP brushes are annealed just below the isotropization temperature for several hours. This is not a purely kinetic effect connected to the LCP's large viscosity but is rather caused by a orientational anchoring at the brush–substrate interface. This interpretation is supported by the observation of a “surface memory effect”,<sup>24</sup> which can be observed at the LC brush coated surfaces. After heating the film to temperatures above the N–I transition ( $T = 120\text{ }^{\circ}\text{C}$ ) for a period from a few seconds to more than half an hour the same patterns are found again upon cooling back into the LC state (parts a and c of Figure 11). Upon close inspection of the micrographs, it is evident that not only is the texture similar to the one before isotropization but also virtually identical domains can be observed, although during heating the LC phase has been completely destroyed (Figure 11b).

The textures even survive immersion of the brush into a good solvent. Figure 11 shows two pictures (parts d and f), taken before and after the brush had been immersed into dichloromethane for 2 h. Dichloromethane is a good solvent for the LC polymer and strongly swells the brush, rendering the surface-attached film completely isotropic (Figure 11e). Clearly, the textures before and after isotropization are identical, and the domain pattern has survived the solvent treatment.

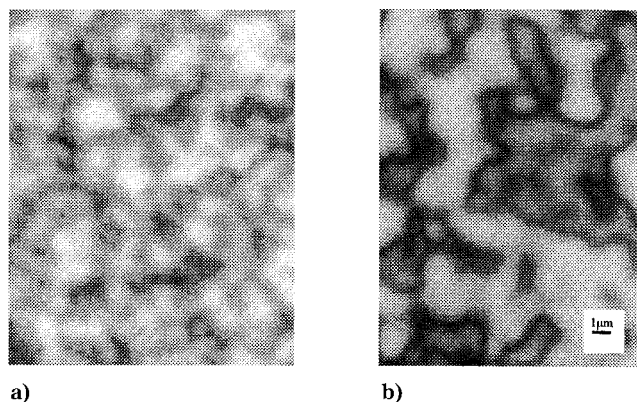


**Figure 12.** Liquid-crystal textures for spin-cast films (sample SC104). When cooled rapidly, the sample has a texture similar to the one observed in brushes (a). When annealed near the transition temperature for 30 min, the texture grows with time (b).

Spin-coated films prepared from the same polymer exhibit a completely different behavior. Figure 12 displays two pictures taken from a spin-cast LCP film with a thickness (104 nm) similar to the brushes described above. When the spin-coated sample is cooled from the isotropic state to room temperature quickly, the domain size is small and is similar to the ones found for brushes (Figure 12a). The average brightness of pictures such as shown in Figure 12 varies sinusoidally with sample orientation. The preferred direction points away from the center of rotation during spin coating and

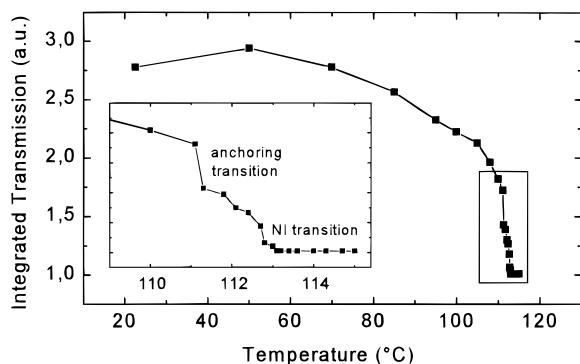


**Figure 13.** Integrated transmission as a function of temperature for sample B61. The inset shows an enlarged view of the range close the NI transition. The anchoring transition at the film-air interface is discernible as a distinct kink.

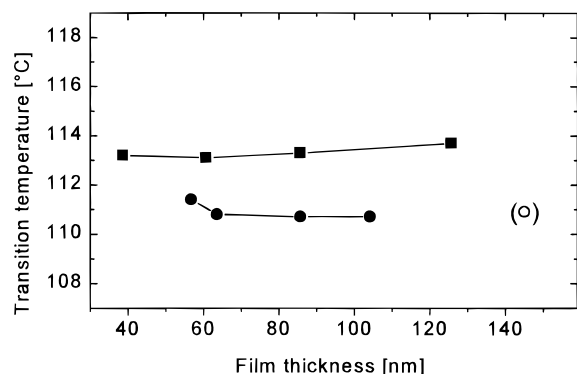


**Figure 14.** Transition temperatures of LC polymers: bulk (○), spin-cast LCP films (●), and LCP brushes (■).

is therefore connected to polymer flow in the early the stages of film formation. In contrast to the behavior of LC brushes the domain size can grow with time when the sample is annealed. Figure 12b was taken after the sample had been annealed near the NI transition temperature for 30 min. A domain structure can still be observed. However, the domains are much bigger than the domains found in brushes, and the domain sizes increase with time as the defects heal. In contrast to the behavior of the brushes, spin-cast LCP films do not memorize their domain pattern after heating to the isotropic state.

The surface memory effect exhibited by the LC brushes is most likely caused by an irregular in-plane orientational anchoring at the interface between substrate and brush. Selection of the in-plane easy axis is caused by rather minor symmetry-breaking anisotropies in the substrate surface, the details of which are poorly understood. Such orienting factors could for example be microscratches or strongly physisorbed mesogenic units.

**Transition Temperatures.** The phase behavior of the brushes is most conveniently demonstrated by plotting the integrated transmission through crossed polarizers vs temperature. Figure 13 shows the intensity vs temperature for a sample with a brush thickness of 61 nm. The N–I transition is clearly observed as a sharp drop of transmitted light. The inset in Figure 13 gives an enlarged view of the transmission behavior close to the transition. The slight kink below  $T_{NI}$ , which is well reproducible in different samples, could be due to an anchoring transition at the brush–air interface.

In Figure 14 the transition temperatures for the different samples are plotted vs film thickness. The

**Table 2. Preparation Conditions of LCP Brushes and Spin-Cast Films**

LCP Brushes				
sample code	thickness (nm) <sup>a</sup>	monomer concn (M)	polym time (h) <sup>b</sup>	$T_{NI}$ (°C) <sup>c</sup>
B126	126	0.99	23.9	113.7
B86	86	0.99	38.2	113.3
B61	61	0.80	44.8	113.1
B38	38	0.80	13.8	113.2

LCP Spin-Cast Films <sup>d</sup>			
sample code	thickness (nm) <sup>a</sup>	speed of rotation (rpm)	$T_{NI}$ (°C) <sup>c</sup>
SC104	104	600	110.7
SC86	86	1000	110.7
SC64	64	1500	110.8

<sup>a</sup> Determined by surface plasmon spectroscopy (SPS) on glass/Ag/SiO<sub>x</sub> substrates. <sup>b</sup> All polymerizations were carried out at 60 °C; toluene was chosen as solvent. <sup>c</sup>  $T_{NI}$  was measured with a polarizing microscope. <sup>d</sup> PM6-4 dissolved in CH<sub>2</sub>Cl<sub>2</sub>; [LCP] = 0.02 mol/L.

conditions for the preparation of the samples are described in Table 1. It is evident that the transition temperature of the brushes does not significantly depend on the film thickness. This is somewhat surprising, because one might have expected that the strong orientational stress exerted by the asymmetric interfaces would destabilize the nematic phase and therefore decrease  $T_{NI}$ .<sup>25</sup>

Interestingly, the transition temperatures  $T_{NI}$  seems to be 2–3 °C higher in the brushes than in the corresponding spin-cast films.  $T_{NI}$  in spin-cast LCP films also depends only weakly on the thickness. It can be excluded that this difference in the  $T_{NI}$  originates from differences between the molecular weight of the brush and the spin-cast polymer from the finding that  $T_{NI}$  depends only very weakly on the molecular weight of the LCP (Table 2). It is possible that chain stretching of the polymer backbone of the brushes stabilizes the nematic phase.<sup>26,27</sup>

## Conclusions

We have synthesized side-chain LCP brushes having thicknesses of up to 200 nm and investigated their optical properties in the dry state. The textures of the brushes observed in the polarizing microscope show domains, which are much larger than the film thickness showing that brush height and LC domain size are not or only weakly correlated. The polarization microscope images of textures contain closed dark lines, which are interpreted as defect walls, possibly arising from conflicting conditions of orientational anchoring at the air and the substrate interface. The domain pattern remains unchanged and reappears after heating the brush to the isotropic phase or even isotropization by exposure to solvent and returning to the LC state. We attribute this surface memory effect to an irregular in-plane orientational anchoring at the brush–substrate interface. We hope to be able to reduce the effect of the surface anisotropies by covering the parts of the substrate not occupied by brush anchors with molecules having long flexible alkyl chains thus decreasing the strength surface anchoring of the LCP. Such experiments are currently underway.

It is interesting to note that the isotropization temperatures of the LCP brushes and of the spin-cast films is also slightly different. The N–I transition tempera-

tures of the LC brushes studied are 2–3 °C higher than those of spin-cast films made from the same polymer, which could be due to chain stretching of the brushes and a concurrent stabilization of the nematic LC phase.

To be used as alignment layers, the LC brushes must swell when brought into contact with a low molecular weight LC. Also, they have to be oriented to macroscopic domains (e.g., through shearing or exposure to an external magnetic field). We will report on the results of such experiments in a subsequent communication.

**Acknowledgment.** The authors thank Friederike Schmid and Avi Halperin for stimulating discussions and Martin Gelbert for help with the analysis of the optical textures. Financial support by the German research council (DFG) is gratefully acknowledged.

## References and Notes

- (1) Jérôme, R. *Rep. Prog. Phys.* **1991**, *54*, 391.
- (2) Yokoyama, H. *Mol. Cryst. Liq. Cryst.* **1988**, *165*, 265.
- (3) Faetti, S. In *Physics of Liquid Crystalline Materials*; Khoo, J. C., Simoni, F., Eds.; Gordon and Breach: Amsterdam, 1991; Chapter XII.
- (4) Uchida, T.; Seki, H. In *Liquid Crystals and Uses*; Bahadur, B., Ed.; World Scientific: Singapore, 1990; Vol. 3, Chapter 5.
- (5) Bahadur, B., Ed. *Liquid Crystals and Uses*; World Scientific: Singapore, 1990.
- (6) Halperin, A.; Williams, D. R. M. *Europhys. Lett.* **1993**, *21*, 575.
- (7) Halperin, A.; Williams, D. R. M. *J. Physics: Condens. Matter* **1994**, *A297*, 6.
- (8) De Gennes, P. G. *J. Phys. (Paris)* **1976**, *37*, 1443.
- (9) Alexander, S. *J. Phys. (Paris)* **1977**, *38*, 983.
- (10) Halperin, A.; Tirell, M.; Lodge, T. P. *Adv. Polym. Sci.* **1991**, *100*, 31.
- (11) Böffel, C.; Spiess, H. W. In *Side Chain Liquid Crystal Polymers*; McArdle, C. B., Ed.; Blackie: Glasgow, Scotland, 1989.
- (12) For a review see: Warner, M. *Phys. Scr.* **1991**, *T35*, 53.
- (13) Prucker, O.; Rühle, J. *Macromolecules* **1998**, *31*, 592.
- (14) Prucker, O.; Rühle, J. *Macromolecules* **1998**, *31*, 602.
- (15) (a) Finkelmann, H.; Ringsdorf, H.; Wendorff, J. H. *Makromol. Chem.* **1978**, *179*, 273. (b) Portugall, M.; Ringsdorf, H.; Zentel, R. *Makromol. Chem.* **1982**, *183*, 2311.
- (16) (a) Rühle, J. *Nachr. Chem. Technol. Lab.* **1994**, *42*, 1237. (b) Rühle, J. *Macromol. Chem. Macromol. Symp.* **1997**, *126*, 215.
- (17) M. Schimmel, Ph.D. Thesis, University of Mainz, 1998.
- (18) Knoll, W. *Makromol. Chem.* **1991**, *192*, 2827.
- (19) See e.g.: G. Odian, *Principles of Polymerisation*, 3rd ed.; Wiley: New York, 1991; Chapter 3.
- (20) De Gennes, P. G.; Prost, J. *The Physics of Liquid Crystals*; Oxford University Press: Oxford, England, 1993.
- (21) Wittebrood, M. M.; Luijendijk, D. H.; Stallinga, S.; Rasing, T.; Musevic, I. *Phys. Rev.* **1996**, *A54*, 5232.
- (22) Ryschenkow, G.; Kleman, M. *J. Chem. Phys.* **1976**, *64*, 404.
- (23) Teixeira, P. I. C.; Sluckin, T. J.; Sullivan, D. E. *Liq. Cryst.* **1993**, *14*, 1243.
- (24) Clark, N. A. *Phys. Rev. Lett.* **1985**, *55*, 292.
- (25) Wittebrood, M. M.; Luijendijk, D. H.; Stallinga, S.; Rasing, Th. *Phys. Rev. E* **1996**, *54*, 5232.
- (26) De Gennes, P.-G. *C. R. Acad. Sci. Paris* **1975**, *281*, 101.
- (27) Schätzle, J.; Kaufhold, W.; Finkelmann, H. *Makromol. Chem.* **1989**, *190*, 3269.
- (28) 300 MHz. Key: s = singlet; b = broad; m = multiplet; d = doublet; t = triplet; q = quintuplet.
- (29) The spectrum of the monomer contains a small signal (x) due to polymer formed by thermal polymerization as no stabilizer was added for the NMR measurements.

MA981474+